Li, X., Ge, M., Dousa, J., Wickert, J. (2014): Real-time precise point positioning regional augmentation for large GPS reference networks. - *GPS Solutions*, *18*, 1, p. 61-71.

DOI: http://doi.org/10.1007/s10291-013-0310-3

Real-time precise point positioning regional augmentation for large GPS reference networks

Xingxing Li[a,b], Maorong Ge[a], Jan Dousa[c], Jens Wickert[a]
a. The German Research Centre for Geosciences (GFZ), Telegrafenberg, 14473 Potsdam, Germany;
lixin@gfz-potsdam.de , maor@gfz-potsdam.de, wickert@gfz-potsdam.de
b. Wuhan University, 129 Luoyu Road, 430079, Wuhan, Hubei, China;
c. Research Institute of Geodesy, Topography and Cartography, Ústecká 98, 250 66 Zdiby, Czech Republic;

Abstract: An increasing number of GNSS reference stations are installed around the world to provide real-time precise positioning services. In most of the current services, a full network solution is required for the precise determination of biases. Such a network solution is time-consuming and difficult to achieve for very large regions such as Europe or China. Therefore, we developed a multi-layer processing scheme for precise point positioning (PPP) regional augmentation to avoid processing large networks. Furthermore we use L1 and L2 raw observations and estimate atmospheric delays, which were properly constrained to the atmospheric corrections derived from the reference stations. Therefore, inaccurate representation of atmospheric delays due to temporal and/or spatial atmospheric fluctuations in the processing can be compensated. The proposed scheme of PPP regional augmentation was implemented into the operational real-time PPP service system at GFZ for validation. The real-time orbit and clock corrections, the uncalibrated phase delays and regional augmentation corrections are generated by this system. The augmentation corrections from the regional network are investigated and the positioning performance in terms of positioning accuracy and time for fixed solution is demonstrated in real-time. Our results indicate that a reliable fixing is possible after five seconds on average. The positioning accuracy is about 12, 10 and 25 mm in east, north and vertical direction, respectively.

Keywords: Real-time Precise Point Positioning; Regional Augmentation; Large Reference Network; Undifferenced Integer Ambiguity; Atmospheric Constraints

1 Introduction

Network-based real-time kinematic (NRTK) positioning with instantaneous ambiguity resolution (Fotopoulos and Cannon 2001; Landau et al. 2007) and real-time precise point positioning (PPP) (Zumberge et al. 1997; Dow et al. 2009) are currently popular techniques for real-time precise positioning. In most of the current NRTK approaches, an integrated solution for all reference stations is carried out in order to provide adequate atmospheric corrections needed for reliable and precise positioning. The generation of such network solution, however, is usually time-consuming and difficult to achieve for large regions such as Europe or China (Bisnath and Gao 2007; Ge et al. 2011). On the contrary, a reliable real-time PPP service can provide precise positioning on a global scale with a worldwide reference network of about 80 stations. But in such a case, PPP needs a comparatively long initialization of about 30 minutes to get centimeter-level positioning accuracy and cannot reach the accuracy of NRTK even after this initial convergence time (Kouba and Hérous 2001; Wang et al. 2002). The PPP performance is expected to improve in the future when more accurate pseudorange measurements will be available or observations at additional carrier frequencies (Feng 2008).

PPP and NRTK have specific advantages and disadvantages. To make use of the first and to reduce the latter both are being further developed and improved. For example, while NRTK developments lead to support undifferenced corrections to extend the service coverage (Zou et al. 2012), several augmentation methods are developed to improve the performance of global PPP service in specific areas by making use of regional reference networks (Wübbena et al. 2005; Li et al. 2011; Zhang et al. 2011a). In the methods developed by Wübbena et al. (2005) and Zhang et al. (2011a), an integrated network solution is still unavoidable which is very time-consuming and seldom available for regional networks with a large number of reference stations.

In this contribution, a multi-layer processing scheme is developed by employing PPP for regional reference stations (Li et al. 2011) in order to avoid processing large networks. Moreover, we use L1 and L2 raw observations in the PPP algorithm and estimate atmospheric delays using proper a priori constraint, so that ambiguities in L1 and L2 can be resolved to integers directly. Consequently, corrections can be generated at the undifferenced level and broadcasted station by station, enabling the user to decide which nearby reference stations should be selected for interpolating the corrections. In this way the heavy communication burden in most of the current NRTK methods can be decreased significantly.

The new processing scheme for PPP regional augmentation (PPP-RA) is implemented into the GFZ real-time precise positioning service system for validation. The performance in terms of the position accuracy and the time to fixed solution is demonstrated with a large set of real-time data.

2 The processing scheme

The observation model for PPP with raw observations is introduced first. A PPP-RA (PPP Regional Augmentation) processing scheme is then proposed for efficient estimation of different corrections. The user positioning algorithm is presented in detail afterwards.

2.1 Observation model

Since the initial phases and hardware delays cannot be easily separated, we group them as uncalibrated phase delay (UPD) for receiver and satellite respectively (Blewitt 1989). Then the observation equations of undifferenced carrier phase and pseudorange can be expressed as

$$L^s_{r,j} = \rho^s_{r\,g} - t^s + t_r + \lambda_j (b_{r,j} - b_j^{\,s}) + \lambda_j N^s_{r,j} - I^s_{r,j} + T^s_r + \varepsilon^s_{r,j} \quad (1)$$

$$P^s_{r,j} = \rho^s_{r\,g} - t^s + t_r + c(d_{r,j} + d_j^{\,s}) + I^s_{r,j} + T^s_r + e^s_{r,j} \quad (2)$$

where indexes s, r and j refer to the satellite, receiver and frequency; t^s and t_r are the clock biases of satellite and receiver; $N^s_{r,j}$ is the integer ambiguity; $b_{r,j}$ and $b_j^{\,s}$ are the receiver and satellite UPDs; λ_j is the wavelength; $d_{r,j}$ is the signal delay from the receiver antenna to the receiver signal correlator; $d_j^{\,s}$ is the signal delay from the satellite signal generator to the satellite antenna; $I_{r,j}^{s}$ is the slant ionospheric delay at the frequency j; T_{r}^{s} is the slant tropospheric delay; $e_{r,j}^{s}$ and $\varepsilon_{r,j}^{s}$ are the pseudorange and carrier phase measurement noise. Furthermore, ρ_g denotes the geometric distance between the electronic phase centers of the satellite and receiver antennas at the signal transmission and receiving epochs. The phase center offsets and variations and the station displacement due to tidal loading must be considered. Other corrections such as phase wind-up or relativistic delays must be precisely applied according to the existing models.

The slant tropospheric delay consists of the dry and wet component. Both can be expressed by their individual zenith delay and mapping function (Boehm et al. 2006). The tropospheric delay is usually corrected for its dry component with an a priori model, e.g. dry Saastamoinen model while the residual part of the tropospheric delay (considered as zenith wet delay Zwd_r) at the station r is estimated from the observations

$$L_{r,j}^{s} = \rho_{r\,g}^{s} - t^{s} + t_{r} + \lambda_{j}(b_{r,j} - b_{j}^{\ s}) + \lambda_{j} N_{r,j}^{s} - I_{r,j}^{s} + Zwd_{r} \cdot M_{r}^{s} + \varepsilon_{r,j}^{s} \tag{3}$$

$$P_{r,j}^{s} = \rho_{r\,g}^{s} - t^{s} + t_{r} + c(d_{r,j} + d_{j}^{\ s}) + I_{r,j}^{s} + Zwd_{r} \cdot M_{r}^{s} + e_{r,j}^{s} \tag{4}$$

where M_{r}^{s} is the wet mapping function.

For multi-frequency observations, the ionospheric delays at different frequency can be expressed as

$$I_{r,j}^{s} = \lambda_{j}^{\ 2} / \lambda_{k}^{\ 2} \cdot I_{r,k}^{s} \tag{5}$$

The ionospheric delays can be eliminated by the linear combination of observations at different frequencies. Usually, the ionosphere-free observation is used for PPP and for the network solution. Alternatively, the dual-frequency data can be processed to also estimate the slant ionospheric delays in the raw observations (Schaffrin and Bock 1988; Odijk 2002). In order to strengthen the solution, a priori knowledge of the ionospheric delays is utilized to constrain the estimated ionospheric parameters. The temporal change in the slant ionospheric delay of a satellite-station pair can be represented by a stochastic process that considers its temporal correlation (Bock et al. 2009; Dai et al. 2003). Ionospheric gradient parameters could be used to represent the spatial character of the ionospheric delay distribution (Chen and Gao 2005). The temporal correlation, spatial characteristics and ionospheric model constraints are comprehensively considered to improve the performance of single-frequency PPP (Shi et al. 2012) and PPP ambiguity fixing (Li, 2012). These constraints, to be imposed on observations of a single station, can be summarized as

$$\begin{aligned} & I_{r,t}^{s} - I_{r,t-1}^{s} = w_t, \quad w_t \sim N(0, \sigma_{wt}^2) \\ & vI_r^s = I_r^s \,/\, f_{r,IPP}^{s} = a_0 + a_1 dL + a_2 dL^2 + a_3 dB + a_4 dB^2, \sigma_{vI}^2 \\ & \tilde{I}_{r,GIM}^{s} = I_r^s, \sigma_{\tilde{I}}^2 \end{aligned} \tag{6}$$

where t is the current epoch and $t-1$ is the previous epoch; w_t is a zero mean white noise with variance σ_{wt}^2; vI_r^s is the vertical ionospheric delay; $f_{r,IPP}^{s}$ is the mapping function at the ionospheric pierce point (IPP); the coefficients $a_i\left(i=0,1,2,3,4\right)$ describe the trend; dL and dB are the longitude and latitude difference between the IPP and the station location , respectively.

2.2 An efficient strategy to derive corrections

Precise positioning service requires that all error components must be represented with certain accuracy in order that errors at the user stations can be mitigated to achieve the desired positioning accuracy. Theoretically, the integrated network solution is an ideal approach which, unfortunately is burdened by a high computational load that increases with the number of network stations. For example, it is very difficult to update satellite clock corrections every second using a network with more than 100 stations. Therefore the integrated network solution is not applicable to regional augmentation of large areas. Taking the various properties of the different error sources into account, we developed a multi-layer processing strategy to avoid the time-consuming network solution for all reference stations. This strategy includes four layers that provide a) precise orbits, b) precise clocks, c) satellite UPDs, and d) ionospheric and tropospheric corrections. The network solution must be used within the first two layers for the estimation of precise satellite orbits and precise clocks. The orbits from the first layer will be fixed for the precise clock estimation in the second layer. In layers three and four the UPDs and ionospheric and tropospheric corrections are generated using PPP and utilizing orbits and clocks derived from the previous layers. The first two layers thus provide the standard products for PPP service as a base. If the capacity of layers three and four is integrated into this base, then

PPP with ambiguity resolution and PPP with regional augmentation can be supported for the user.

The precise orbit is usually determined in a batch-processing mode using about 100 globally distributed stations Due to its dynamic stability it is predicted for real-time applications. The GFZ provides an ultra-rapid product (GFU) updated every three hours for real-time users. The clock corrections have to be estimated and updated much frequently (Zhang et al. 2011b) due to their short-term fluctuation. The clock corrections can be estimated with the same or a similar network as used for the orbit determination or with a regional network consisting at least of tens of stations. During clock estimation the satellite orbit and station coordinates are held fixed or are tightly constrained while the satellite and receiver clocks, the ambiguities and the ZTD parameters are estimated. Strong constraints on fixed double-differenced ambiguities would also enhance the solution and improve the accuracy of the estimated clock products (Geng et al. 2012).

The UPDs estimates from a dense reference network are more stable and accurate than when estimated from a sparse network (Geng et al. 2011; Li and Zhang 2012). With precise orbit and clock products, the UPDs can be estimated using ambiguities from the PPP solution (Ge et al. 2008), which enables UPD to be estimated from much denser networks. In this contribution, we also employ the raw observation equations of (3), (4), (5) and ionospheric constraints of (6) to derive the UPDs on L1 and L2 frequency instead of using Melbourne-Wübbena (MW) and ionosphere-free (L3) combinations.

One possible solution for achieving instantaneous ambiguity-fixing is to provide precise atmospheric delay corrections as is done in NRTK. Since the ionosphere and troposphere are spatially correlated with correlation reducing with distance, dense reference networks with an inter-station baselines of several tens of kilometers are required for the precise representation of atmospheric delays. This is also the major reason for deploying more than 300 stations in Germany and over 1000 stations in China to provide NRTK services.

The key for a precise representation of all the biases is a successful ambiguity resolution of the regional reference network (Li et al. 2011; Zou et al. 2012). With the orbit and clock products available, and using the undifferenced observations (3) and (4), the relation (5), and ionospheric constraints (6), the PPP solution can be carried out station by station. For all regional reference stations the coordinates can be fixed to speed up the convergence time. By applying the L1 and L2 UPD corrections from layer 3, the integer ambiguity resolution can be attempted at any epoch in real-time. As soon as most of the undifferenced integer (UD) ambiguities are fixed to integers, the undifferenced atmospheric corrections can be derived straightforwardly. With the integer UD-ambiguities of the reference network, the corresponding undifferenced atmospheric corrections of ionospheric slant delay and zenith wet delay can be derived station by station as

$$I^s_{r,j} - Zwd_r \cdot M^s_r = \rho^s_{r\,g} - L^s_{r,j} - t^s + t_r + \lambda_j (b_{r,j} - b_j^{\,s}) + \lambda_j N^s_{r,j} + \varepsilon^s_{r,j} \quad (7)$$

$$-I^s_{r,j} - Zwd_r \cdot M^s_r = \rho^s_{r\,g} - P^s_{r,j} - t^s + t_r + c(d_{r,j} + d_j^{\,s}) + e^s_{r,j} \quad (8)$$

This procedure is very easy to be realized even for the reference network with a large number of stations. Furthermore, biases with different physical characteristics such as tropospheric and ionospheric delays can also be represented separately at the server-end for possible improvement based on their own properties. Besides the significant improvement in the computational efficiency, it is also of great importance that the corrections can be broadcasted station by station via NTRIP (Networked Transport of RTCM via Internet Protocol, http://igs.bkg.bund.de/ntrip). A number of nearby reference stations can be selected by a user according to the approximate coordinates and relevant station-wise atmospheric corrections can be disseminated efficiently. The heavy communication burden in most of the current NRTK methods can be reduced significantly in this way.

2.3 Positioning Algorithm

At the user-end, the same PPP algorithm described by (3) to (5) is utilized. Using the orbit and clock corrections only, the standard PPP can be carried out. If any UPD product is also available, the PPP ambiguity fixing can be achieved on a global scale based on tens of minutes of observations. Furthermore, if the precise atmospheric corrections from a regional reference network are also accessible via NTRIP, the user can achieve almost instantaneous ambiguity-fixing by applying the interpolated corrections for removal of atmospheric delays.

However, the atmospheric delays derived at each station could be biased due to an inaccurate modeling or other station-dependent error since the lower-order polynomial interpolation might not be able to represent irregular spatial and temporal fluctuations in small scales. This representation error could be reduced by deploying very dense reference networks. In order to balance the representation accuracy and the density of reference stations, the ionospheric slant delay and tropospheric zenith delay at the user stations are estimated as unknown parameters similar to the standard PPP using (3) to (5) and properly constrained to the interpolated corrections. In this way, the standard PPP and augmented PPP can also be integrated.

Assume that the selected reference stations are r_1 to r_n for interpolating corrections for user r_u. The ionospheric slant delay parameter for an individual satellite s_i is constrained to the interpolated correction as

$$I_{r_u}^{s_i} - \tilde{I}_{r_1,r_2\cdots r_n}^{s_i} = w_I, \quad w_I \sim N(0, \sigma_{w_I}^2) \tag{9}$$

and the constraint for the zenith wet delay parameter is

$$Zwd_{r_u} - \tilde{Z}wd_{r_1,r_2\cdots r_n} = w_T, \quad w_T \sim N(0, \sigma_{w_T}^2) \tag{10}$$

where $I_{r_u}^{s_i}$ denotes the slant ionospheric delay from station r_u to satellite s_i ; $\tilde{I}_{r_1,r_2\cdots r_n}^{s_i}$ is the interpolated ionospheric correction ; Zwd_{r_u} denotes the zenith wet delay for station r_u , and $\tilde{Z}wd_{r_1,r_2\cdots r_n}$ is the interpolated correction. The biases between the true and the interpolated corrections w_I and w_T are zero mean white processes with variance of $\sigma_{w_I}^2$ and $\sigma_{w_T}^2$ for ionospheric and tropospheric delays, respectively.

3 The PPP-RA Service System

The EPOS-RT software (Ge et al. 2011) has been developed in the IGS (International GNSS Service) real-time data analysis center at GFZ and is used for generating real-time orbits, clocks, global ionospheric map (GIM) and UPD. Recently, the software was adapted for providing regional augmentation corrections (RAC) and the corresponding client software iPPP extended for using these RACs. The new system is now running operationally to provide RACs for Germany with the SAPOS real-time stations.

The data flow at the server of the PPP-RA service is illustrated in Fig. 1. The server receives data from the observation caster for both global and regional stations. The global data is employed to estimate orbits and clocks which are transmitted via the service caster to users. With the orbits and clocks data, the PPP can be carried out for any reference station, so that UPD can be estimated from the ambiguities of the PPP solutions. With the orbits, clocks and UPDs data being available, the integer UD ambiguities on L1 and L2 frequency are fixed in PPP mode and atmospheric corrections are derived and casted to users on a station basis. It should be mentioned that ambiguity resolution at the regional reference stations is very critical, as an ionospheric correction can be derived only when its ambiguity is fixed. This is also shown in (7).

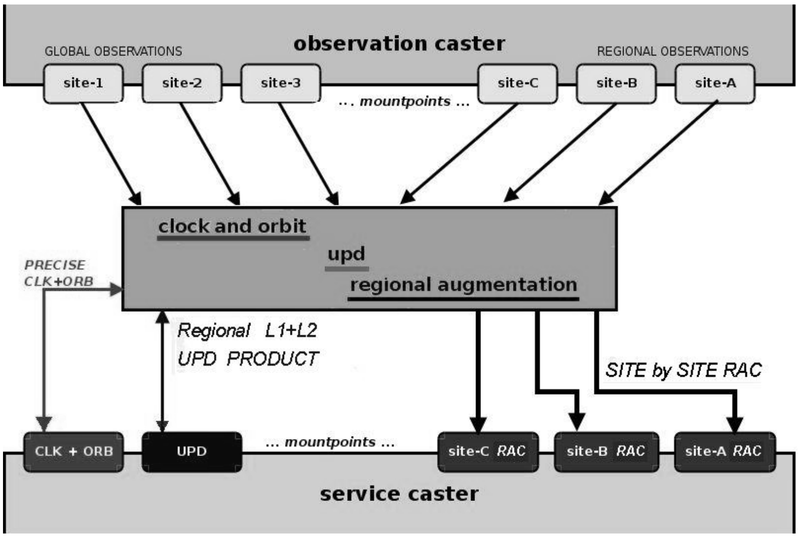

Fig. 1 Data flow at the server of the PPP-RA service.

At the user stations, the source table with the regional reference station locations should be downloaded at the beginning. At least three nearby stations are selected according to the user location and the communication link is setup for continuously receiving corrections. Besides the orbit, clock and UPD products used in PPP ambiguity resolution, the atmospheric corrections must be interpolated and imposed as constraint on related parameters. Then the instantaneous ambiguity resolution is achievable. The data flow at the user is illustrated in Fig. 2.

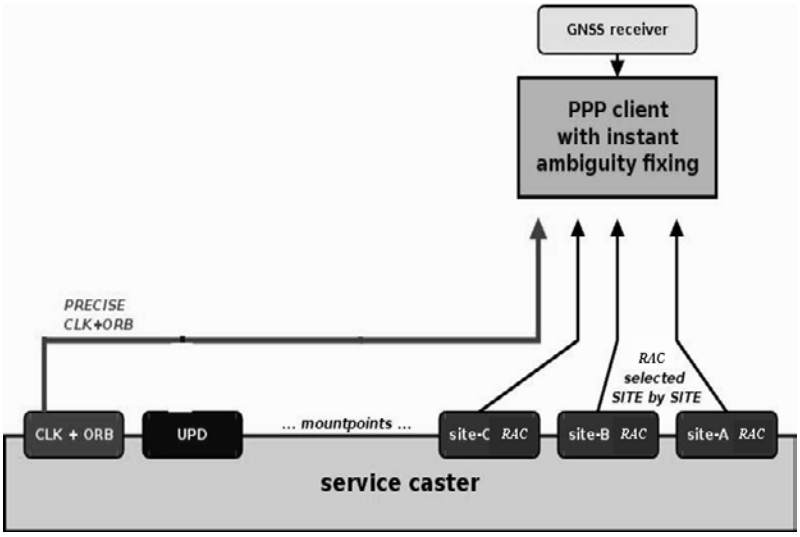

Fig. 2 Data flow at the user end for PPP-RA using regional augmentation corrections.

4 Results

The positioning results are analyzed to validate the performance. Both, real-time positioning accuracy and time to achieve a fixed solution are evaluated using a large data set.

4.1 Data and Processing Strategy

Fig. 3 shows the distribution of the German SAPOS real-time stations. There are about 300 stations (small red dots), equipped with various types of GNSS receivers. The real-time data with 1Hz sampling rate is provided for this study. The real-time orbit and clock products are generated as described in Section 2.2. The selected regional reference stations (large black dots) are processed in PPP mode using the generated orbit and clock products, and UPDs are then estimated from these regional stations. The UD atmospheric corrections are generated on the selected regional reference stations by using the strategy introduced in Section 2.2. The corrections are broadcasted via NTRIP on the station basis.

Seventeen stations which are marked with green squares are chosen as test stations. The user positioning algorithm, as presented in Section 2.3, was applied at each test station. Three nearby reference stations are selected for interpolating corrections and a cut-off elevation angle of 10° is applied to ensure usable observations. The station coordinates are estimated epoch by epoch without any constraints between epochs. The integer ambiguity resolution is attempted epoch-wise and L1 and

L2 ambiguities are fixed simultaneously using the LAMBDA method (Teunissen 1995). The ratio between the minimum and the second minimum quadratic form of residuals is applied to decide about the success of fixing the integer ambiguity candidate while the threshold for the ratio test is set to three as usual.

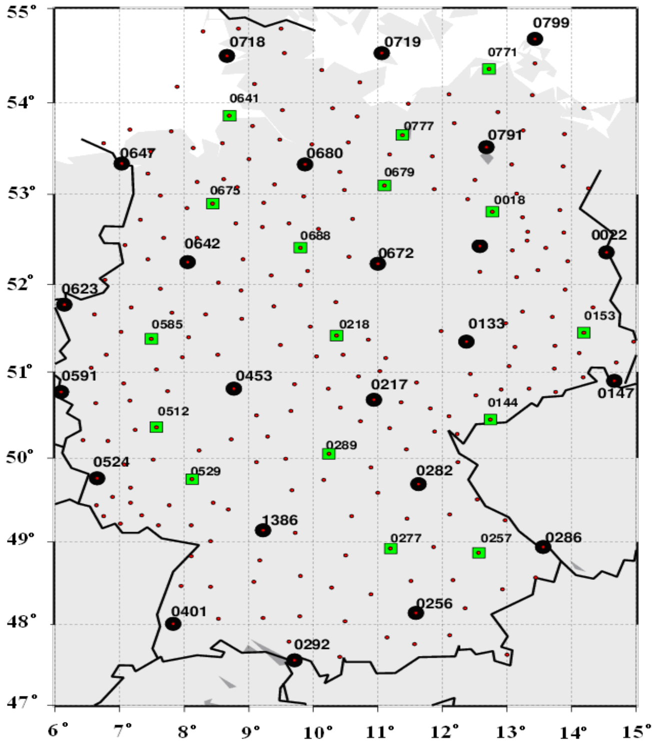

Fig. 3 Distribution of real-time stations of the SAPOS network used for this study. Each small red dot indicates a station. Large black dots indicate the selected regional reference stations and the large squares refer to for user stations.

4.2 PPP-RA Performance

For the selected user stations, the estimator is restarted every minute to obtain the statistics on the time for ambiguity-fixing and the position accuracy of the fixed solution. The statistical results of GPS week 1675 are shown in Figs. 4 to 6. Fig. 4 shows the statistics of the observation time needed for successful ambiguity fixing. For about 87% of the solution the ambiguity can be fixed with just one epoch of data. On average, data of five seconds are needed for a reliable ambiguity-fixing. We also notice that there are few solutions where ambiguities cannot be fixed within the predefined restarting time of one minute. Further investigation should be carried out for possible improvement.

As soon as the integer ambiguities have been successfully fixed, the coordinates at the epoch are used to assess the positioning accuracy of the PPP-RA service. The fixed solutions are compared with the precise coordinates from post-processed daily solutions. Fig. 5 shows the distribution of position differences in up direction. The vertical component has a RMS of 25 mm. Fig. 6 shows the distribution of position differences in horizontal direction. The RMS of east and north components are 12 mm and 10 mm respectively.

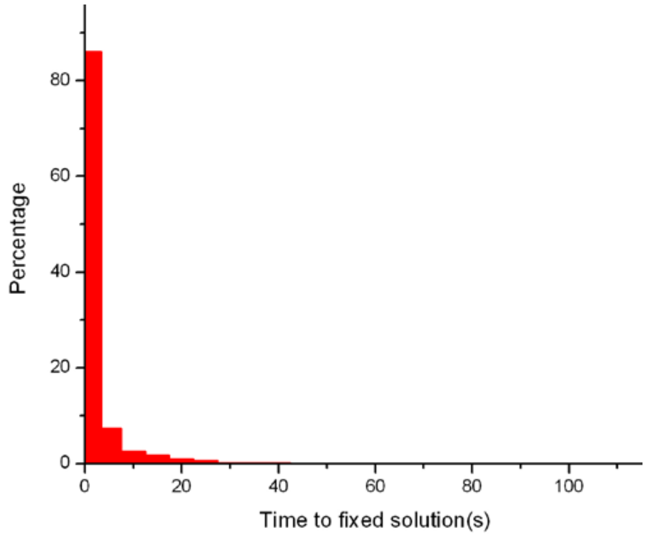

Fig. 4 Observing time needed for ambiguity-fixing

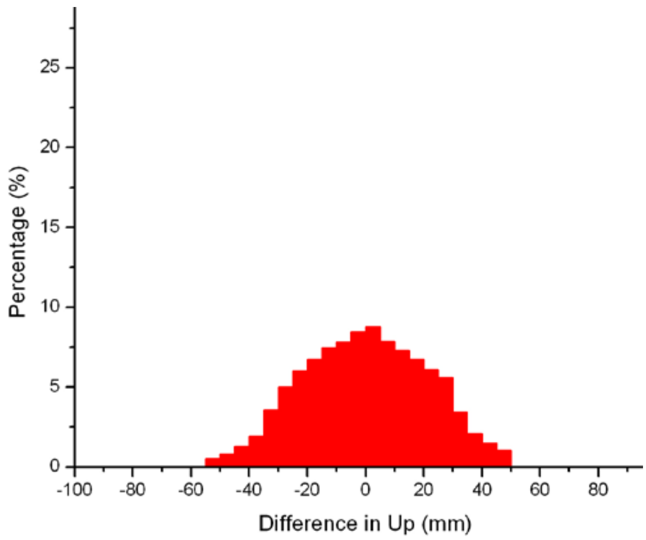

. Fig. 5 Distribution of position errors in the vertical component.

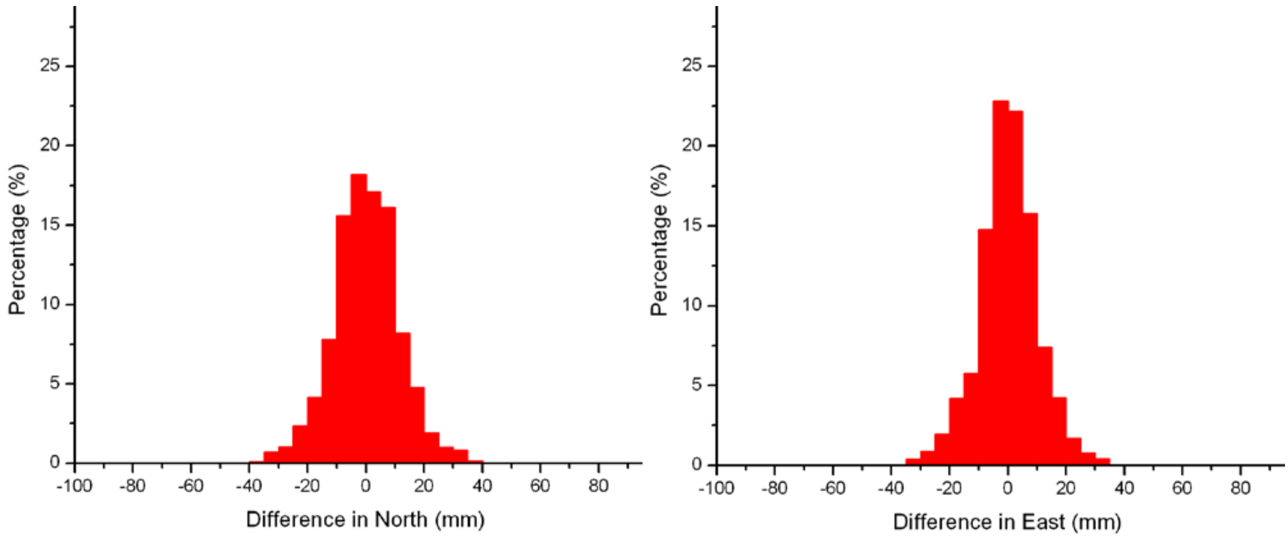

Fig. 6 Distribution of position errors in the horizontal components.

For validating the improvement of the PPP algorithm using raw observations, the PPP-RA scheme by Li et al. (2011), in which user observations are corrected directly with atmospheric corrections and wide-lane/ionosphere-free observations are employed, is also carried out in parallel. The corresponding results are shown in Figs. 7 to 9. Fig. 7 shows the statistics of observation time needed for successful ambiguity fixing. For about 68% of the solutions the ambiguity can be fixed with one epoch of data. On average, data of ten seconds are needed for a reliable ambiguity-fixing. Fig. 8 shows the distribution of position differences in the up direction. The vertical component has a RMS of about 30 mm. The RMS of east and north components (Fig. 9) are 15 and 12 mm, respectively. These results confirm that the new PPP algorithm significantly improves the ambiguity fixing performance and positioning accuracy.

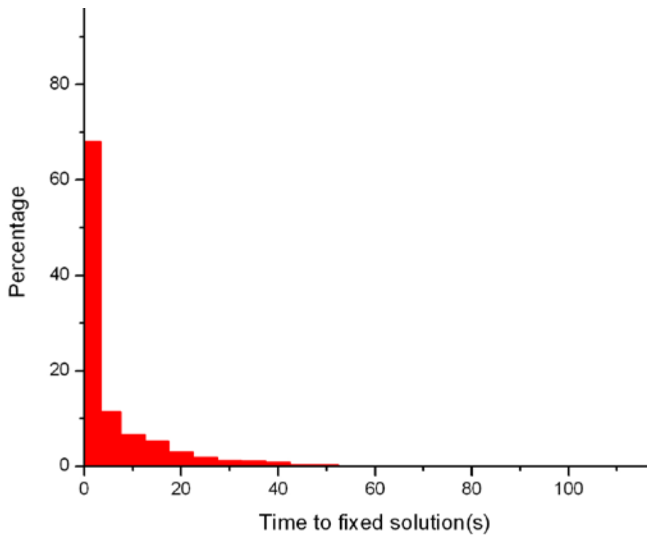

Fig. 7 Observing time needed for ambiguity-fixing.

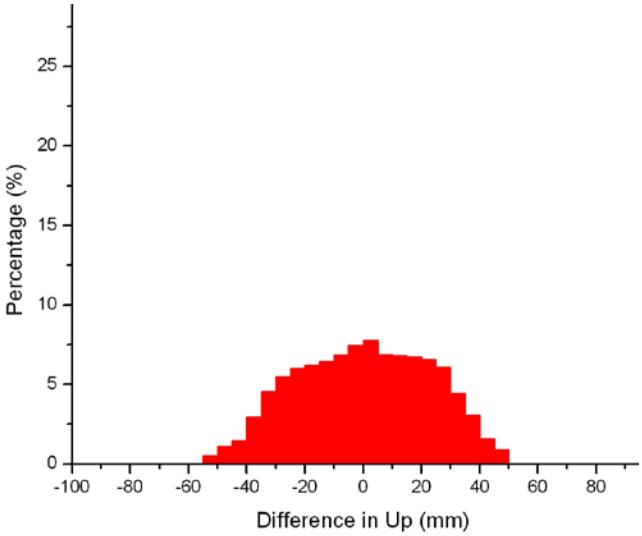

Fig. 8 Distribution of the position errors in the vertical component.

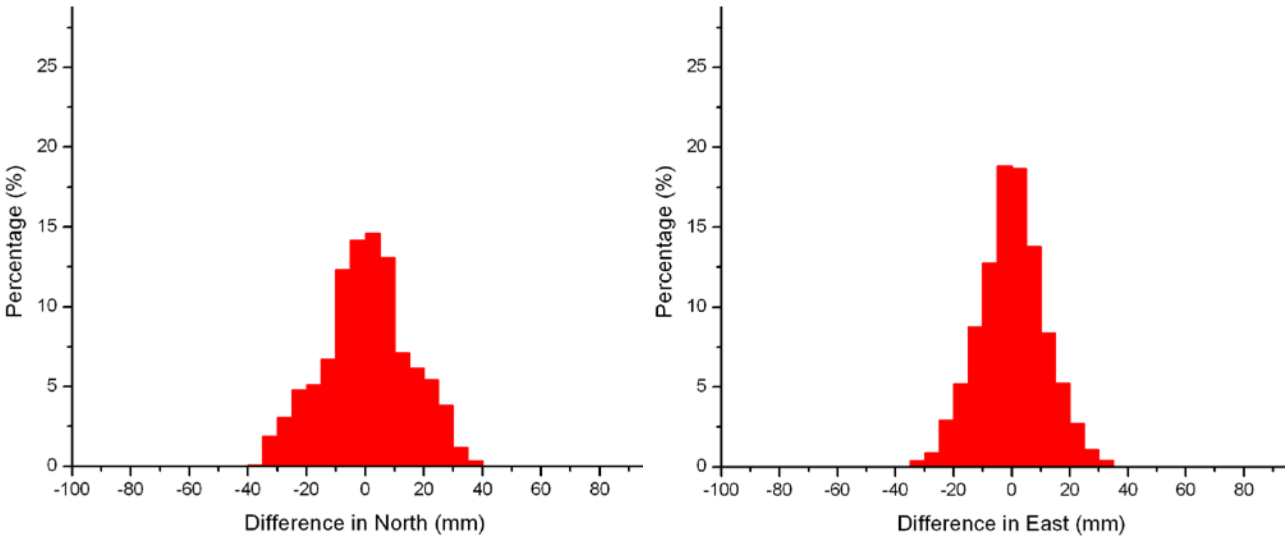

Fig. 9 Distribution of the position errors in the horizontal components.

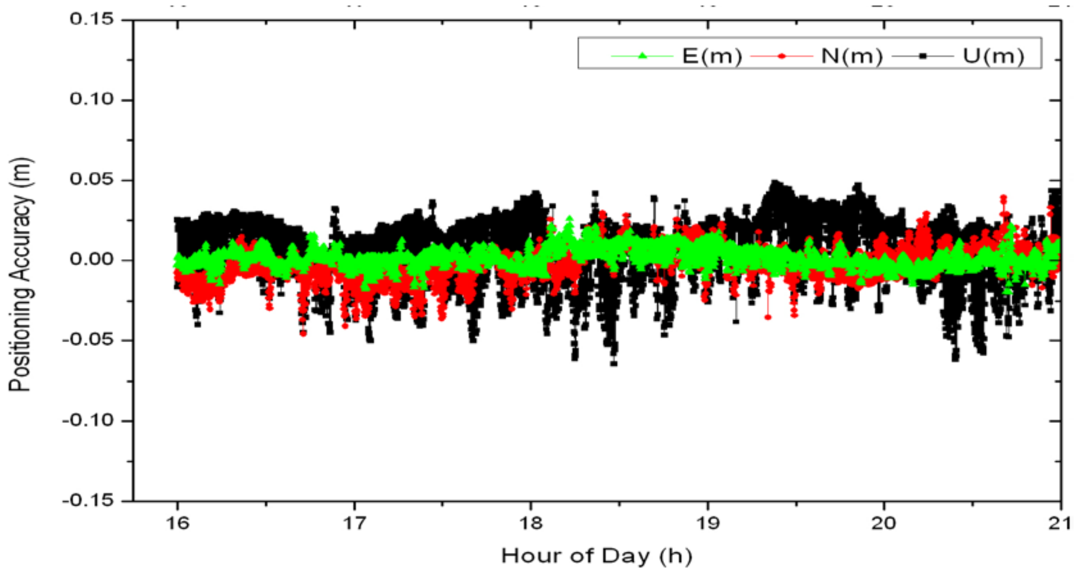

Fig. 10 Positioning errors at the station 0675 on DOY 43, 2012

An example for the position differences of fixed kinematic PPP solution and post-processed daily solution for the SAPOS station 0675 is given in Fig. 10. This figure indicates that a position accuracy of a few centimeters is achievable using PPP with regional augmentation corrections.

4.3 Investigation on corrections

To better understand the level of improvement, reached by the application of the new strategy, we selected stations 0642, 0647, 0680 and 0675. The UD corrections and the interpolated values were derived and analyzed in detail.

The estimated UD ionospheric delays and the corresponding elevation angles of GPS satellite PRN15 are illustrated as an example in Fig. 11 for one continuous arc from 16:00 to 21:00 on February 12, 2012 (DOY 043). One can see the temporal correlation of the ionospheric delay and the strong correlation between elevation angles and ionospheric delays. The zenith wet delays of the SAPOS station 0642 are shown in Fig. 12.

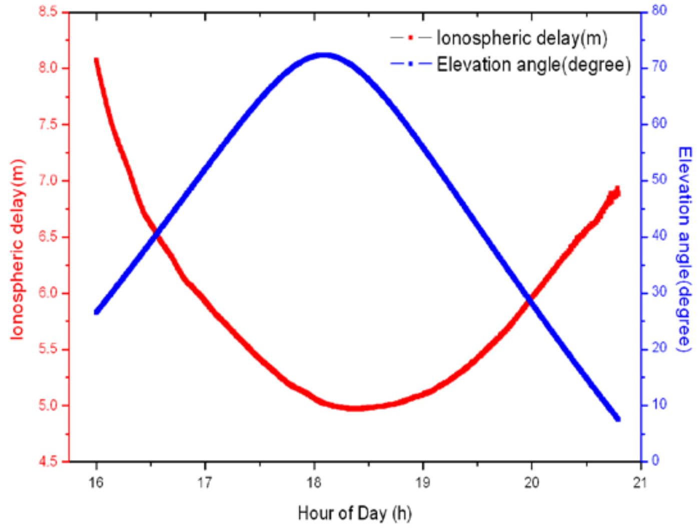

Fig. 11 Ionospheric delays and elevations for satellite PRN15 at station 0642 during 16:00 to 21:00

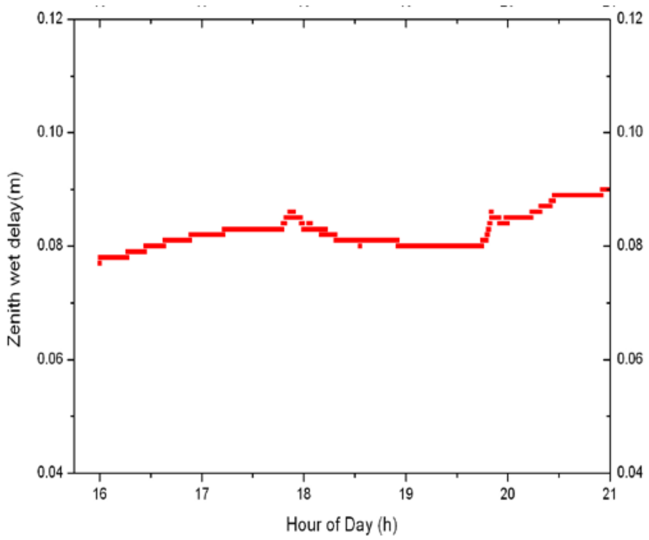

Fig. 12 Zenith wet delays at station 0642 from 16:00 to 21:00

Typical uncalibrated phase delays of GPS satellite PRN15 on L1 and L2 frequencies are shown in Fig. 13 while the corresponding UPDs of wide-lane (WL) and narrow-lane (NL) combinations are shown in Fig. 14. We can observe that the real-time UPDs are stable enough for a few hours, and the WL UPDs are stable over even a much longer interval.

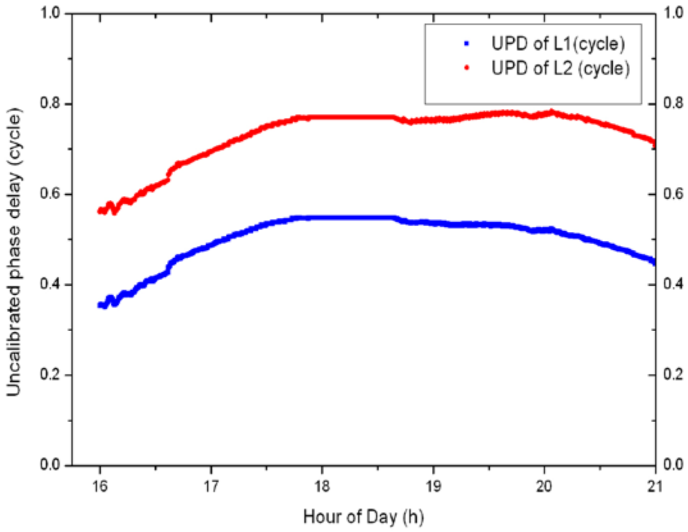

Fig. 13 Uncalibrated phase delays of satellite PRN15 on L1 and L2 frequencies

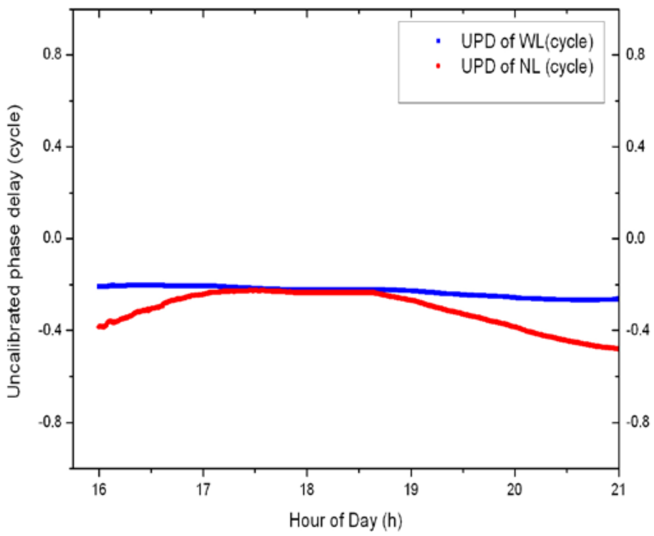

Fig. 14 Uncalibrated phase delays of satellite PRN15 on WL and NL combinations

With the UD atmospheric delays retrieved at the augmentation stations 0642, 0647 and 0680, the atmospheric delays of user station 0675 are interpolated epoch by epoch with the linear combination method. The resulting interpolations are compared with the retrieved values as was done similarly at the reference stations in order to assess the accuracy of the interpolation. Fig. 15 shows the differences for satellite PRN15, the differences are seen to be generally smaller than 5 cm with RMS of 2 cm. Tropospheric interpolation errors are shown in Fig. 16. Since the accuracy of zenith wet delay interpolation is better than 1 cm, the corrections are accurate enough for rapid ambiguity fixing.

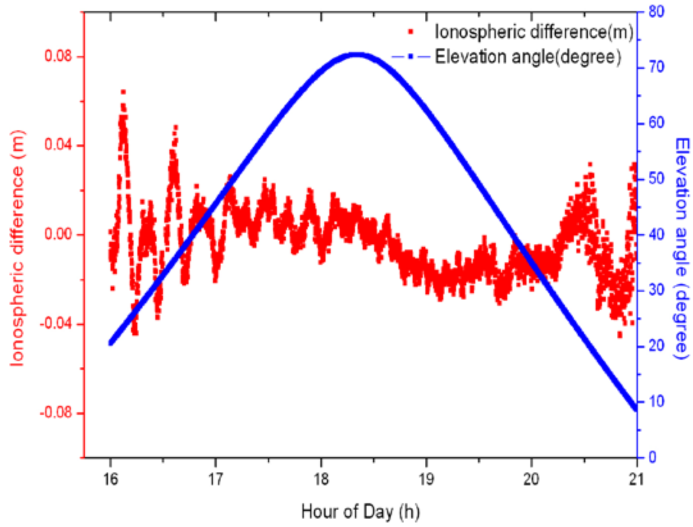

Fig. 15 Ionospheric modeling errors and elevation angles of PRN15 at station 0675

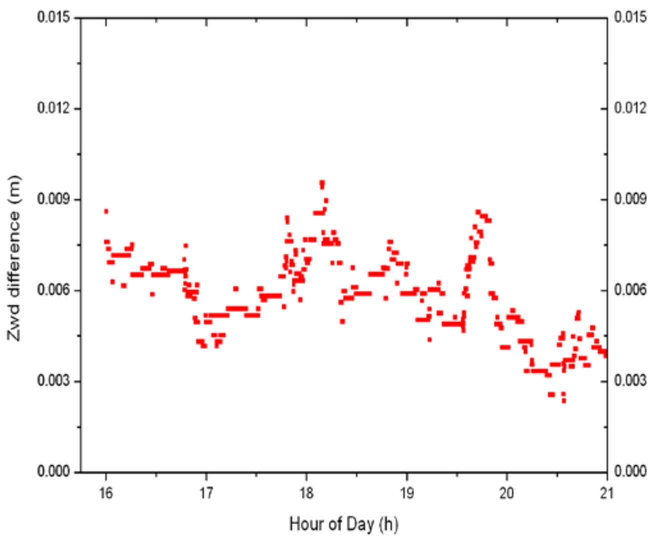

Fig. 16 ZWD modeling errors at station 0675

5 Conclusions

A multi-layer strategy for precise GNSS data processing was developed and introduced in order to realize PPP augmentation with a large number of reference stations. The generation of orbits and clocks as incorporated in the current real-time PPP system at GFZ are included as two basic layers. This makes it possible that PPP can be utilized for any station, including the regional reference stations, in the other two layers that pertain to the estimation of UPDs and regional augmentation corrections.

At each reference station, the integer ambiguity on L1 and L2 frequency are fixed in PPP mode by using raw observations. Once most of the UD-ambiguities of the reference stations are resolved, the corresponding undifferenced atmospheric corrections can be derived and broadcasted station by station to users.

The atmospheric delays, derived at each station could be biased due to inaccurate modeling or station-dependent error, and the lower-order polynomial interpolation might not be able to represent irregular spatial and temporal fluctuations of small scales. Therefore, we use L1 and L2 raw observations with atmospheric delay parameters which are constrained properly to the interpolated atmospheric corrections. A proper constraint, which matches the accuracy of corrections, can compensate the remaining systematic biases caused by large inter-station distances.

The new PPP-RA scheme is implemented into the EPOS-RT software and is running operationally at GFZ to demonstrate the positioning performance in accuracy and time for fixed solutions. The statistics show that ambiguities can be fixed with just one epoch of data in about 87% of the cases, and five seconds are needed on average for reliable ambiguity-fixing. After ambiguity fixing, the RMS of the PPP position differences, compared to the daily static solution, is about 12, 10 and 25 mm in east, north and vertical components, respectively.

Acknowledgements

We thank the International GNSS Service and SAPOS Germany with its central office for providing real-time data for this study. The authors would also like to give their special thanks to Dr. Jake Griffiths and an anonymous reviewer. Their valuable comments and suggestions improved the manuscript greatly.

6 References

Bisnath S, Gao Y (2007) Current state of precise point positioning and future prospects and limitations. Observing our changing Earth, International Association of Geodesy Symposia 133, Springer-Verlag Berlin Heidelberg, pp. 615–623

Blewitt G (1989) Carrier phase ambiguity resolution for the global positioning system applied to geodetic baselines up to 2,000 km. J Geophys Res 94(B8):10187-10203. doi:10.1029/97JB03534

Bock H, Jäggi A, Dach R, Schaer S (2009) GPS single-frequency orbit determination for low Earth orbiting satellites. Adv in Space Res, 43(5): 783-791

Boehm J, Niell A, Tregoning P, Schuh H (2006) Global Mapping Function (GMF): A new empirical mapping function based on numerical weather model data. Geophys. Res. Lett. 33, L7304, doi: 10.1029/2005GL025546

Chen K, Gao Y (2005) Real-Time Precise Point Positioning Using Single Frequency Data. Proceedings of ION GNSS-2005, September 2005, Long Beach, CA, pp.1514-1523

Dai L, Wang J, Rizos C (2003) Predicting atmospheric biases for real-time ambiguity resolution in GPS/GLONASS reference station networks. J Geod. 76(11/12), 617-628

Dow JM, Neilan RE, and Rizos C (2009) The International GNSS Service in a changing landscape of Global Navigation Satellite Systems, J Geod, 83(3/4):191-198, DOI: 10.1007/s00190-008-0300-3

Feng Y (2008) GNSS three carrier ambiguity resolution using ionosphere-reduced virtual signals. J Geod, 82(12):847-862

Fotopoulos G., Cannon M (2001) An overview of multi-reference station methods for cm-level positioning. GPS Solutions, 4(3), 1-10

Ge M, Gendt G, Rothacher M, Shi C, Liu J (2008) Resolution of GPS carrier-phase ambiguities in precise point positioning(PPP) with daily observations. J Geod 82(7):389-399. doi:10.1007/s00190-007-0187-4

Ge M, Dousa J, Li X, Ramatschi M, Wickert J (2011), A Novel Real-Time Precise Positioning Service System: Global Precise Point Positioning with Regional Augmentation, in: Proceedings of the 3rd Int. Colloquium - Galileo Science, 31 August - 2 September 2011, Copenhagen, Denmark

Geng J, Teferle F, Meng X, and Dodson A (2011) Towards PPP-RTK: Ambiguity resolution in real-time precise point positioning. Adv in Space Res, 47 (10) 1664-1673

Geng J, Shi C, Ge M, Dodson AH, Lou Y, Zhao Q, Liu J (2012), Improving the estimation of fractional-cycle biases for ambiguity resolution in precise point positioning, J. Geod. , 86(8):579–589, doi:10.1007/s00190-011-0537-0

Kouba J, Hérous P (2001) Precise point positioning using IGS orbit and clock products. GPS Solutions 5(2):12-28. doi:10.1007/PL00012883

Landau H, X Chen, S Klose, R Leandro, U Vollath (2007) Trimble's RTK and DGPS Solutions in Comparison with Precise

Point Positioning, Observing our Changing Earth, International Association of Geodesy Symposia 133, Proceedings of the 2007 IAG General Assembly, Perugia, Italy, July 2–13, pp. 709-718

Li X, Zhang X, Ge M (2011) Regional reference network augmented precise point positioning for instantaneous ambiguity resolution. J. Geod., 85(3):151-158, Doi: 10.1007/s00190-010-0424-0

Li X, Zhang X (2012) Improving the Estimation of Uncalibrated Fractional Phase Offsets for PPP Ambiguity Resolution. J. Navig. 65(3):513-529 doi:10.1017/S0373463312000112

Li X (2012) Improving Real-time PPP Ambiguity Resolution with Ionospheric Characteristic Consideration. Proc. of ION GNSS-12, Institute of Navigation, Nashville, Tennessee, September,17-21

Odijk D (2002) Fast precise GPS positioning in the presence of ionospheric delays. Netherlands Geodetic Commission, Publications on Geodesy, Vol 52, pp. 242

Schaffrin B, Bock Y (1988) A unified scheme for processing GPS dual-band phase observations. Bull. Geod. 62(2):142-160

Shi C, Gu S, Lou Y, Ge M (2012) An improved approach to model ionospheric delays for single-frequency Precise Point Positioning. Adv in Space Res, 49(12):1698–1708

Teunissen PJG (1995) The least squares ambiguity decorrelation adjustment: a method for fast GPS integer estimation. J. Geod., 70(1/2): 65-82

Wang J, Satirapod C, Rizos C (2002) Stochastic assessment of GPS carrier phase measurements for precise static relative positioning. J. Geod., 76(2):95-104

Wübbena G., Schmitz M., Bagge A (2005) PPP-RTK: precise point positioning using state-space representation in RTK network, Proc. of ION GNSS-05, Institute of Navigation, Inc., Fairfax, USA, pp. 2584–2594

Zhang B, Teunissen PJG, Odijk D (2011a) A novel undifferenced PPP-RTK concept. J. Navig. , 64(S1):S180-S191 doi:10.1017/S0373463311000361

Zhang X, Li X, Guo F (2011b) Satellite Clock Estimation at 1 Hz for Realtime Kinematic PPP applications. GPS Solutions 15(4): 315-324, doi: 10.1007/s10291-010-0191-7

Zou X, Ge M, Tang W, Shi C, Liu J (2012) URTK: undifferenced network RTK positioning. GPS Solutions (Online First), doi: 10.1007/s10291-012-0277-5

Zumberge JF, Heflin MB, Jefferson DC, Watkins MM, Webb FH (1997) Precise point positioning for the efficient and robust analysis of GPS data from large networks. J Geophys Res 102(B3):5005-5017. doi:10.1029/96JB03860

Biography (about 50 words per author)

Mr. Xingxing Li is a Ph.D. student at the Department of Geodesy and Remote Sensing of the German Research Centre for Geosciences (GFZ). He holds a B.S. degree in Geodesy and Geomatics from Wuhan University in China. His current research focuses on the development of real-time GNSS precise positioning techniques.

Dr. Maorong Ge received his PhD in Geodesy at Wuhan University, Wuhan, China. He is now a senior scientist at the German Research Center for Geosciences (GFZ Potsdam). He was technically in charge of the IGS Analysis Center and is now leading the development of the GNSS real-time software EPOS-RT at GFZ. His research interests are GNSS algorithms and software development.

Jan Douša received his PhD in geodesy from the TU Prague in 1999. Since 2000 he has been at the Geodetic Observatory Pecný (GOP) of the Research Institute of Geodesy, Topography and Cartography for precise GNSS applications including strategies and software developments. He is responsible for GOP analytical contributions to the IGS (precise ultra-rapid orbits), the EUREF (European reference frame), and the E-GVAP project (global and European near real-time zenith tropospheric delay estimations) .

Dr. Jens Wickert graduated in physics from the Technical University Dresden and obtained his doctor degree in 2002 from the Karl-Franzens-University Graz in Geophysics/Meteorology. He worked in atmospheric research for several German Research Institutes before starting in GNSS science in 1996. He is deputy head of the section “GPS/Galileo Earth Observation” at the German Research Center for Geosciences GFZ at Potsdam. Dr. Wickert is involved in many national and international satellite missions and research projects.